

Fe²⁺ sorption onto nontronite (NAu-2)

Deb P. Jaisi^{a,b,*}, Chongxuan Liu^c, Hailiang Dong^a, Ruth E. Blake^b, Jeremy B. Fein^d

^a Department of Geology, Miami University, Oxford, OH 45056, USA

^b Department of Geology and Geophysics, Yale University, P.O. Box 208109, New Haven, CT 06520, USA

^c Pacific Northwest National Laboratory, Richland, WA 99352, USA

^d Department of Civil Engineering and Geological Sciences, University of Notre Dame, Notre Dame, IN 60432, USA

Received 10 December 2007; accepted in revised form 27 August 2008; available online 17 September 2008

Abstract

The sorption of ferrous iron to a clay mineral, nontronite (NAu-2, a ferruginous smectite), was investigated under strictly anoxic conditions as a function of pH (3–10), Fe²⁺ concentration (0.01–50 mM), equilibration time (1–35 days), and ionic strength (0.01–0.5 M NaClO₄). The surface properties of NAu-2 were independently characterized to determine its fixed charge and amphoteric site density in order to interpret the Fe²⁺ sorption data. Fe²⁺ sorption to NAu-2 was strongly dependent on pH and ionic strength, reflecting the coupled effects of Fe²⁺ sorption through ion exchange and surface complexation reactions. Fe²⁺ sorption to NAu-2 increased with increasing pH from pH 2.5 to 4.5, remained constant from pH 4.5 to 7.0, increased again with further increase of pH from pH 7.0 to 8.5, and reached a maximum above pH 8.5. The Fe²⁺ sorption below pH 7.0 increased with decreasing ionic strength. The differences of Fe²⁺ sorption at different ionic strengths, however, diminished with increasing equilibration time. The Fe²⁺ sorption from pH 4.5 to 7.0 increased with increasing equilibration time up to 35 days and showed stronger kinetic behavior in higher ionic strength solutions. The kinetic uptake of Fe²⁺ onto NAu-2 is consistent with a surface precipitation mechanism although our measurements were not able to identify secondary precipitates. An equilibrium model that integrates ion exchange, surface complexation and aqueous speciation reactions reasonably well describes the Fe²⁺ sorption data as a function of pH, ionic strength, and Fe²⁺ concentration measured at 24 h of equilibration. Model calculations show that the species Fe(OH)⁺ was required to describe Fe²⁺ sorption above pH 8.0 satisfactorily. Overall, this study demonstrated that Fe²⁺ sorption to NAu-2 is affected by complex equilibrium and kinetic processes, likely caused by surface precipitation reactions.

© 2008 Elsevier Ltd. All rights reserved.

1. INTRODUCTION

Iron is the fourth most abundant element in Earth's crust and is ubiquitous in clays and clay minerals (Horne, 1978; Stucki, 2006). Iron-containing clay minerals are important in nutrient cycling, contaminant retention and migration and acid/base buffering (Baeyens and Bradbury, 1997; Stucki et al., 2002; Stucki, 2006). Clay mineral properties are, in part, controlled by the redox state of iron

(Anastacio et al., 2005). The iron redox couple (Fe²⁺/Fe³⁺) controls the oxidation/reduction potential in many anoxic and semi-anoxic environments (Grenthe et al., 1992). For example, Fe²⁺ is an important reductant in a variety of natural anoxic environments such as lakes, ground water, ocean basins, unconsolidated and swamp sediments, hydromorphic soils and engineered systems (Charlet et al., 1998; Amonette, 2003; Strathmann and Stone, 2003; Fredrickson et al., 2004; Hofstetter et al., 2006). The concentration of Fe²⁺/Fe³⁺ species in these environments is controlled by their sorption properties and by the formation and stability of Fe-containing mineral phases (Liger et al., 1999; Peretyazhko and Sposito, 2005).

The sorption properties of different clay minerals have been extensively studied for a wide range of metals and

* Corresponding author. Address: Department of Geology and Geophysics, Yale University, P.O. Box 208109, New Haven, CT 06520, USA. Fax: +1 203 432 3134.

E-mail address: deb.jaisi@yale.edu (D.P. Jaisi).

contaminants in subsurface environments (Baeyens and Bradbury, 1997; Turner et al., 1998; Zachara et al., 2002; Bradbury and Baeyens, 2005). Previous studies of the uptake of metals such as Ni, Co, Zn onto clay mineral surfaces have found that metal precipitates can form even if the metal concentration is under-saturated with respect to their pure oxy(hydro)oxide form (Scheidegger et al., 1998; Thompson et al., 1999; Schlegel et al., 2001). Incorporation of metals and neof ormation of phyllosilicates have been found to occur depending on the reaction kinetics dictated by specific chemical conditions (Schlegel et al., 2001; Dähn et al., 2002, 2003; Schlegel and Manceau, 2006). However, the mechanisms of Fe^{2+} interaction with clay minerals is still poorly documented (Tournassat and Charlet, 2002; Schultz and Grundl, 2004; Tournassat et al., 2004; Charlet and Tournassat, 2005; Géhin et al., 2007; Jaisi et al., 2007a; Merola et al., 2007), despite the fact that Fe^{2+} is the most reactive species for the reduction of a wide variety of both organic and inorganic contaminants (Chisholm-Brause et al., 1994; Stumm and Morgan, 1996; Charlet et al., 1998; Liger et al., 1999; Hofstetter et al., 2006; Zachara et al., 2007; Jaisi et al., 2008). Fe^{2+} sorption is extremely sensitive to trace oxygen and requires the establishment and maintenance of fully anoxic conditions during experimental investigations. Such strictly anoxic systems have been developed recently using an oxygen trap (Jeon et al., 2004) or an effective oxygen scavenger such as cysteine (Logan et al., 2005).

Here, we report an investigation of Fe^{2+} sorption onto the clay mineral nontronite (NAu-2) in a strictly anoxic environment. NAu-2 (a ferruginous smectite) was selected for this research primarily because Fe^{3+} in its structure (Keeling et al., 2000; Gates et al., 2002) can be biologically or chemically reduced to Fe^{2+} (Li et al., 2004; Jaisi et al., 2005, 2007a,b), and because the surface-complexed Fe^{2+} has been found most reactive among different Fe^{2+} species associated with NAu-2 in reduction and immobilization of groundwater contaminants (Jaisi et al., 2008). We investigated Fe^{2+} sorption to NAu-2 as a function of pH, ionic strength, equilibration time, and Fe^{2+} concentration under strictly anoxic conditions. Properties of the fixed charge and amphoteric surface sites of NAu-2 were independently characterized in order to interpret the Fe^{2+} sorption data. A model that links surface complexation, ion exchange, and Fe^{2+} aqueous speciation reactions was developed in order to explain the observed sorption behaviors.

2. MATERIALS AND METHODS

2.1. Mineral, media and reagent preparation

2.1.1. Chemicals and experimental supplies

All solutions and suspensions were prepared with Millipore Milli-Q 18 M Ω water. NaOH and HCl stock solutions were made from reagent grade chemicals for all experiments except for the potentiometric titrations, for which commercially supplied volumetric standards were used (see Section 2.2). Fe^{2+} stock solutions were prepared from analytical grade FeCl_2 salt. All experimental vials were washed with 0.05 M H_2SO_4 and Milli-Q water, and

were kept inside an anaerobic glove box for at least 2 weeks before any experiments involving Fe^{2+} were performed.

Plastic bottles for all experiments were acid-washed with heated 8 M HNO_3 and glassware was washed with 20% HNO_3 and rinsed with Milli-Q water. Polypropylene bottles (100 or 500 mL) were used for preparing stock solutions and 20-mL glass vials were used for subsequent sorption experiments. All glassware, plasticware and syringes were kept inside an anaerobic glove box for at least a week prior to use.

2.1.2. Clay mineral preparation

Bulk nontronite (NAu-2 : $\text{M}_{0.72}^+(\text{Si}_{7.55}\text{Al}_{0.45})(\text{Fe}_{3.83}\text{Mg}_{0.05})\text{O}_{20}(\text{OH})_4$, where M is the interlayer cation (Ca, Na, K); Keeling et al., 2000), was purchased from the Source Clays Repository, IN. The sample was sonicated briefly in order to disperse loosely aggregated particles, and then centrifuged to obtain a size fraction of 0.02–0.5 μm . The treated particles were characterized by direct current plasma (DCP) emission spectroscopy, chemical extractions, X-ray diffraction (XRD) and transmission electron microscopy (TEM) and scanning electron microscopy (SEM) with energy dispersive spectrometry (EDS) for mineralogy and morphology. The treated NAu-2 was pure nontronite, with no other detectable mineral phases or impurities. The details of the mineralogical and chemical characterizations of NAu-2 are discussed in Keeling et al. (2000) and Gates et al. (2002).

To prepare homoionized NAu-2 in Na, the pure NAu-2 sample was treated by repetitive ion exchange (4 times) in aqueous 1.0 M NaClO_4 solution (Bukka et al., 1992; Baeyens and Bradbury, 1997; Bradbury and Baeyens, 2005; Hofstetter et al., 2006). Such homoionization effectively removes residual sparingly soluble minerals (if any) such as calcite that may have been present in the original NAu-2 (~1%; Keeling et al., 2000) and trace cation impurities that could potentially influence the sorption results (Bradbury and Baeyens, 2005; Rabung et al., 2005). Each of the repetitive ion exchange treatments was carried out for a period of 24 h with constant, slow stirring at room temperature. The exchanged NAu-2 was dialyzed with Milli-Q water for a week, introducing fresh water twice a day in order to wash out any residual cations and perchlorate. The dialyzed NAu-2 was freeze-dried and stored until further analysis.

The cation exchange capacity of the 0.02–0.5 μm fraction of NAu-2 was 697(\pm 73) mmol/kg as determined from the NH_4^+ exchange method (Sumner and Miller, 1996). The surface area of the same size fraction of NAu-2 measured by BET- N_2 adsorption was 33.5 m 2 /g.

2.2. Potentiometric titrations

Potentiometric titrations of the 0.02–0.5 μm suspension of NAu-2 at a concentration of 1.3 g/L were carried out under a N_2 atmosphere at 298 K in either 0.01, 0.1, or 0.5 M NaClO_4 . The NAu-2 suspension was saturated in a given ionic strength electrolyte for 48 h before the titration. The titration experiments were performed with an automated burette assembly, and pH measurements were made with a glass combination electrode filled with 4 M KCl. The elec-

trode was calibrated with commercially supplied pH standards (from pH 2.0 to 10.0).

Electrolyte titrations were performed in order to determine the point of zero net proton charge (pH_{PZNPC}) (Sposito, 1984; Liu et al., 2007) of NAu-2. For this purpose, NAu-2 was equilibrated in 0.01 M NaClO₄ for 24 h by maintaining a constant pH of 7.0 using 0.01 M HCl or NaOH. Aliquots of pH-stabilized NAu-2 suspension were placed in separate vials and then adjusted to a desired pH value (5–9) using 0.1 or 0.01 M HCl or NaOH. The final concentration of NAu-2 was adjusted to 1.3 g/L. The ionic strength of the solution was then increased to 0.5 M using NaClO₄ salt. The stabilized pH after 24 h of equilibration was measured. The difference in pH (Δ pH) due to the addition of NaClO₄ was plotted as a function of initial pH. The pH_{PZNPC} was determined at Δ pH = 0.

Acid–base titrations were started from the pH_{PZNPC} and advanced towards either acidic or basic pH. Results were then merged to obtain an entire titration curve. Trial titration experiments were performed in order to identify the optimal NAu-2 concentration and pH ranges to minimize artifacts such as those from mineral dissolution (Schulthess and Sparks, 1986), and the dissolved solutes were quantified by ICP-MS. All titration experiments were carried out by adding a commercially supplied volumetric standard of 0.1 M HCl and 0.1 M NaOH in a NaClO₄ background electrolyte solution. The nontronite suspension was purged with nitrogen gas for 60 min. prior to the titration experiment, and was kept under a nitrogen gas atmosphere during the experiment in order to exclude CO₂ gas from the experimental solutions.

2.3. Fe²⁺ sorption experiments

Batch sorption experiments were performed in order to measure the Fe²⁺ sorption as a function of pH (2.6–10.8), equilibration time (1–35 days), and Fe²⁺ concentration (0.01–50 mM). The sorption pH edge of Fe²⁺ onto NAu-2 was determined at a fixed concentration of Fe²⁺ (330 μ M) and NAu-2 (1.3 g/L) with the equilibration time varying from 1 to 35 days to determine the kinetic behavior of Fe²⁺ sorption. Mineral dissolution was monitored for all experimental pH values both with and without added Fe²⁺. Sorption as a function of Fe²⁺ concentration was determined at a constant NAu-2 concentration (1.3 mg/mL) and pH (7.0 \pm 0.2) after 24 h of equilibration.

All sorption experiments were conducted in duplicate in an anaerobic glove box (96% N₂ and 4% H₂, Coy Laboratory, Ann Arbor, MI) in which the oxygen partial pressure (pO₂) was continuously monitored with an O₂ sensor. The NAu-2 stock solution was prepared and stored in the glove box for seven days, but the Fe²⁺ stock solution (from FeCl₂) was prepared inside the glove box before the experiments and was kept in a dark, Al-foil wrapped container. Once the required amount of acid/base was added to attain a target pH value, the suspension was allowed to equilibrate for a desired time and the final stable pH was measured. All experimental tubes were equilibrated by continuous mixing (60 rpm) at 30 °C.

Phase separation was carried out by centrifugation throughout this work. The total Fe²⁺ concentration [Fe_{tot}²⁺] was measured by treating the whole sample with 1 M Ultrex HCl at a 1:1 ratio for 24 h followed by Ferrozine assay (Stookey, 1970). Aqueous [Fe_{aq}²⁺] concentrations were measured on supernatants obtained after centrifugation of the suspensions followed by Ferrozine assay. The concentration of sorbed Fe²⁺ was calculated as the difference between the total [Fe_{tot}²⁺] and the aqueous [Fe_{aq}²⁺] concentration (in μ mol/L).

3. RESULTS

3.1. Anoxic experimental conditions

The anoxic condition was monitored in all experiments by determining the stability of Fe²⁺ (at 330 μ M) as a function of time both in aqueous (i.e. without sorbent) and sorbed (to NAu-2) phases in parallel to Fe²⁺ sorption experiments. Electrolyte solutions that were prepared in the anaerobic glove box normally contained less than 1 ppm of O₂. The trace O₂ was removed by adding 15 μ M (final concentration) of cysteine (Logan et al., 2005). Extensive pre-tests were performed to determine an optimal concentration of cysteine that was sufficient to consume trace O₂ to undetectable levels and yet was low enough not to effect Fe²⁺ stability and Fe²⁺ sorption to NAu-2. The effect of cysteine on Fe²⁺ sorption was indirectly evaluated by measuring the sorption of Ni²⁺, a redox inactive analogue of Fe²⁺, onto NAu-2 in solutions with and without 15 μ M cysteine. The influence of cysteine on Ni²⁺ sorption was undetectable at the cysteine concentrations used in the Fe²⁺ experiments, suggesting that cysteine likely exerted no effect on the extent of Fe²⁺ sorption. The O₂ level in the final experimental vials was determined using a CHEMets[®] colorimetric analysis kit R-7540 (2.5 ppb sensitivity). The measurement of Fe²⁺ in the control experiments showed that 96(\pm 1.2)% and 100% of Fe²⁺ remained in the sorbed and aqueous phases, respectively, after 35 days of equilibration. We conclude, therefore, that the Fe²⁺ sorption experiments were conducted under strictly anoxic conditions and that no Fe²⁺ was oxidized within the detection limits (\sim 10 μ M).

3.2. Dissolution of NAu-2 at low and high pH

The concentrations of dissolved Si, Al, Mg, and Fe continuously increased with time during the sorption experiments indicating the dissolution of NAu-2 (Fig. 1a). The dissolution proceeded at all pH values and increased with increasing or decreasing pH with the strongest dissolution in the pH regions of <3.5 and >9.5 (Fig. 1b). These results are generally consistent with those of Furrer et al. (1993) and Zysset and Schindler (1996) who measured dissolution of montmorillonite as a function of pH. The dissolution data were used to select the optimal pH range for the potentiometric titration experiments in order to avoid significant NAu-2 dissolution during the titrations.

The changes in the concentrations of dissolved cations as a function of time were similar for all major elements

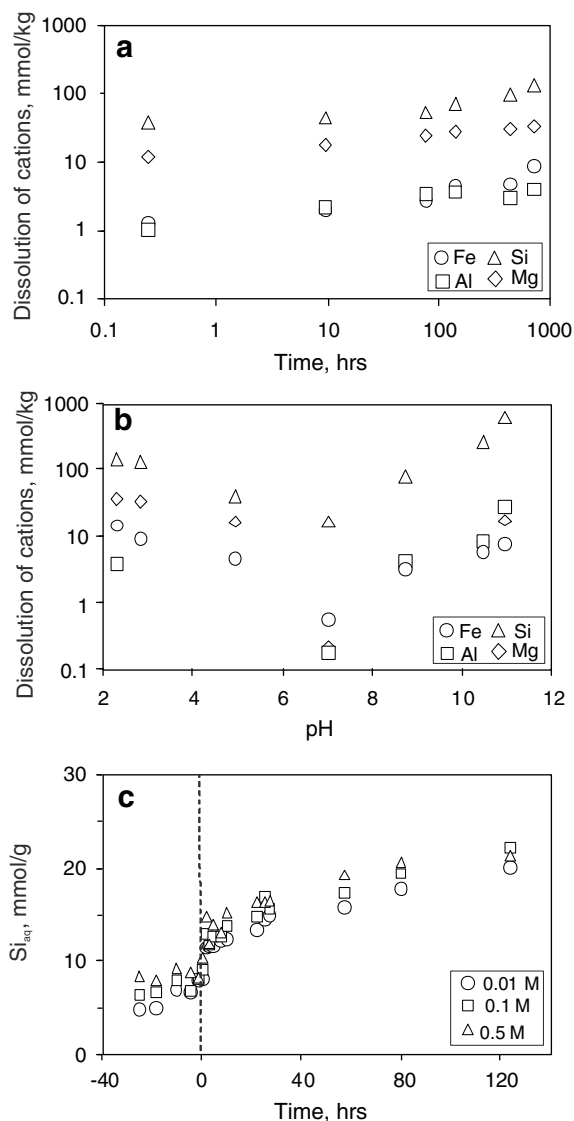


Fig. 1. (a) Dissolution of structural cations measured in solution as a function of time at pH 2.84; (b) function of pH after 715 h of equilibration; and (c) kinetics of Si release before and after Fe²⁺ addition (dotted line).

(Si, Al, Mg, Fe) at both acidic and basic pH. Based on the extent of dissolution at pH 2.84, the dissolution rate of NAu-2 was estimated to be 5.08×10^{-12} mol/g-s (or 1.5×10^{-13} mol/m²-s). This rate of dissolution is close to that reported by Amram and Ganor (2005) (2.8×10^{-12} mol/g-s) and Golubev et al. (2006) (6.2×10^{-12} mol/g-s) for smectites. It is interesting to note that our observed rate of dissolution of nontronite is within the same order of magnitude as that of smectite, despite differences in the mineral structures, experimental conditions (batch vs. flow-through) and solution chemistry (Amram and Ganor, 2005; Metz et al., 2005; Golubev et al., 2006). The measured rate of dissolution, when converted to the extent of NAu-2 mass loss (ca. 0.02%, 0.1%, 0.31% and 0.72% in 1, 5, 15 and 35 days, respectively) was insignificant relative to the amount of NAu-2 present over the time frame of the

Fe²⁺ sorption experiments. However, the presence of dissolved ions from nontronite dissolution significantly affected the experimental solution chemistry in the long-term sorption experiments.

When the measured concentrations of dissolved cations (Fig. 1a and b) were normalized with respect to their concentrations in the NAu-2 structure, the order of their release to aqueous solution was Mg > Si > Al > Fe, suggesting incongruent dissolution of NAu-2. This result is consistent with those of May et al. (1986) and Stumm and Wieland (1990) who have shown that clay minerals dissolve incongruently and release structural elements such as Al, Fe, Si, and Mg both at low and high pH values. The observed rates of dissolved ion release may have also been affected by cation exchange or surface complexation reactions, which can selectively remove ions from solution (Zysset and Schindler, 1996).

The Si dissolution data at pH 7.0 (Fig. 1c) show an increase in the dissolution rate immediately after Fe²⁺ addition. This rate increase lasted only for 2–3 h. The rate of Si dissolution after this time remained almost constant. This increase in the dissolution of structural cations when other bivalent metal cations are added is consistent with several publications that suggest that metal sorption onto mineral surfaces can destabilize surface metal ions (such as Si, Mg and Fe in NAu-2) relative to the bulk mineral (Scheidegger et al., 1998; Schlegel et al., 1999). The extent of such increased Si dissolution in our experiments (~10 μ mol/g) is within the same order of magnitude as that found for hectorite (21 μ mol/g; Schlegel et al., 1999).

3.3. Electrolyte and potentiometric titration

The point of zero net proton charge (pH_{PZNPC}) determined from electrolyte titration was at pH 7.2 (Fig. 2). This pH_{PZNPC} is higher than that of montmorillonite and illites (Lebron et al., 1993) but lower than that of smectites (Kriaa et al., 2007). However, the value of the pH_{PZNPC} has been found to vary extensively among different clay minerals (ca. Table 1, Kriaa et al., 2007).

All potentiometric titration data are expressed in terms of moles of protonated/deprotonated sites per mass of NAu-2 (mmol/kg) (e.g., Fein et al., 2005):

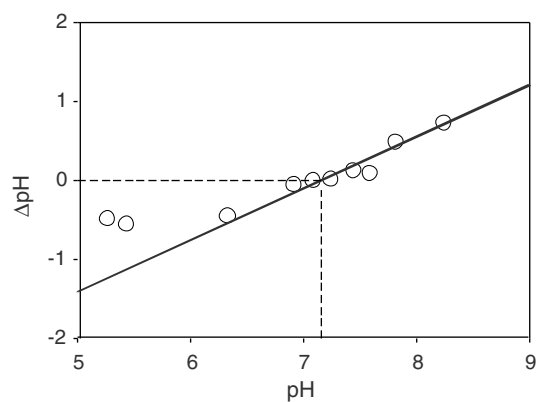


Fig. 2. Electrolyte titration of NAu-2. The pH_{PZNPC} for NAu-2 (ΔpH = 0) was observed at pH 7.2.

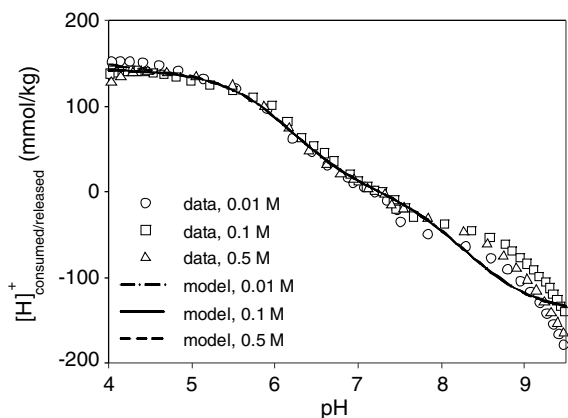


Fig. 3. Total acid/base titration of conditioned NAu-2 as a function of ionic strength of the background electrolyte at 0.01, 0.1 and 0.5 M NaClO₄ (symbols) and corresponding model fits (lines). NAu-2 was equilibrated for 48 h in the electrolyte and stabilized to pH_{PZNPC} before each acid/base titration.

$$[\text{H}^+]_{\text{consumed/released}} = \frac{1}{m_{\text{NAu-2}}} (C_a - C_b - [\text{H}^+] + [\text{OH}^-]) \quad (1)$$

where C_a and C_b are the concentrations of acid and base added at each step of titration; brackets represent species concentrations (protons or hydroxyl ions), and $m_{\text{NAu-2}}$ is the concentration of NAu-2 (g/L).

The titration curves normalized to NAu-2 mass vary only slightly as a function of electrolyte concentration (0.01, 0.1,

and 0.5 M NaClO₄) (Fig. 3). Similar results have been reported by Baeyens and Bradbury (1997). Only data from pH 4.0 to 9.5 are reported because of the observed incongruent dissolution of NAu-2 precluded reliable measurements at lower and higher pH values (Fig. 1). The concentration of net protons consumed below the pH_{PZNPC} nearly converges at different ionic strengths and reaches a maximum plateau below pH 4.5. The nearly constant proton consumption from pH 4 to 4.5 suggests that the amphoteric sites are saturated with protons under these conditions. The average proton consumption obtained from titration endpoints (pH 4–4.5) was 141.8 (±7.0) mmol/kg (or 4.2 ± 0.2 μmol/m²) of NAu-2 in the 0.01–0.5 M electrolyte solutions. This site density is higher than published values such as 82–95 mmol/kg for SWy-1 montmorillonite (Stadler and Schindler, 1993; Baeyens and Bradbury, 1997), 79 mmol/kg for KGa-2 kaolinite (Heidmann et al., 2005) and 92.4 mmol/kg for hectorite (Schlegel et al., 1999). The site density of 141.8 mmol/kg was used to describe Fe²⁺ sorption to the amphoteric sites in the following modeling analysis (see Section 4.3).

3.4. Fe²⁺ sorption pH edge

Fe²⁺ sorption as a function of pH at three different electrolyte concentrations (0.01, 0.1 and 0.5 M of NaClO₄) (Fig. 4) show that Fe²⁺ sorption onto NAu-2 is pH dependent. The percentage of sorbed Fe²⁺ sharply increases with increasing pH to pH 4.5, followed by a more shallow increase with increasing pH to 7.0, and then a steeper increase again to pH 9.0, above which the sorption reaches

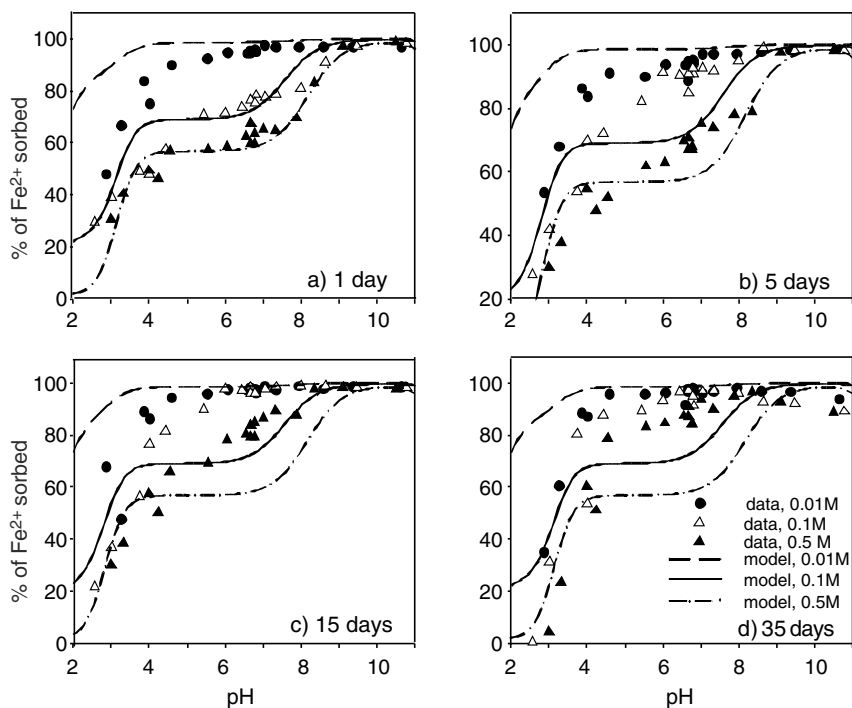


Fig. 4. Fe²⁺ sorption edge for the conditioned NAu-2 as a function of pH and electrolyte concentration. The experiment was performed for (a) 1 day; (b) 5 days; (c) 15 days and (d) 35 days. The experiments were performed at three ionic strengths of the background electrolyte (0.01, 0.1 and 0.5 M NaClO₄). The points represent the experimental data and the lines represent modeling results. The model fitted results from day 1 (a) are included in (b–d) for comparison only.

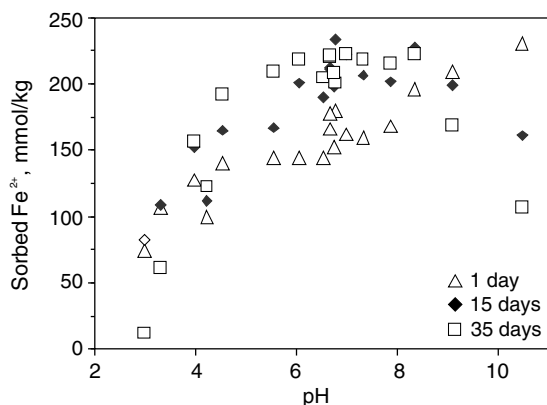


Fig. 5. Effect of acidic and basic pH on the dissolution of NAu-2 during Fe^{2+} sorption in 0.5 M NaClO_4 . The data are the same as those depicted in Fig. 4.

a maximum. Increasing ionic strength decreases Fe^{2+} sorption below pH 8.0, with the most profound influence between pH 4.5 and 8.0.

The Fe^{2+} sorption edge varies with time and the extent of variation is dependent on ionic strength (Fig. 4). In 0.01 M solution, the extent of Fe^{2+} sorption only slightly varies from 1 to 35 days of equilibration, indicating that Fe^{2+} sorption reaches equilibrium within 24 h. In 0.1 and 0.5 M solutions, however, the sorbed Fe^{2+} at pH 4.5–8.0 continuously increases with time from 1 to 35 days of equilibration, indicating a kinetic behavior of Fe^{2+} sorption onto NAu-2. As described in Section 4.1 (Fig. 1c), the longer term kinetics most likely results from slow surface nucleation/precipitation. Below pH 4.5 and above pH 8.0, the temporal changes to Fe^{2+} sorption are relatively minor. Near pH 3 and 10, however, the sorbed Fe^{2+} at 35 days of equilibration is lower than that at other times (Fig. 5), indicating desorption of sorbed Fe^{2+} with time at these pH values. For example, at the end of 35 days of equilibration, 18.7% and 12.5% of Fe^{2+} desorbed at pH 3 and 10, respectively, compared to that of sorbed Fe^{2+} at 1 day of equilibration. The decreased Fe^{2+} sorption with increasing equilibration time apparently results from the dissolution of NAu-2, which releases cations (Fig. 1) that subsequently compete with Fe^{2+} for sorption sites on NAu-2. Under these conditions, the interplay of several complex reactions such as sorption, desorption and precipitation of sorbate, bulk mineral dissolution, selective sorption and/or precipitation of dissolved ions may occur concurrently at different rates.

3.5. Fe^{2+} sorption isotherm

The sorption isotherm is expressed as a distribution ratio (K_d) as a function of the corresponding aqueous Fe^{2+} concentration (Fig. 6):

$$K_d = \frac{(\text{Fe}_0^{2+} - \text{Fe}_{\text{aq}}^{2+}) / m_{\text{NAu-2}}}{\text{Fe}_{\text{aq}}^{2+} / V}, \quad (2)$$

where Fe_0^{2+} is the initial Fe^{2+} concentration, $\text{Fe}_{\text{aq}}^{2+}$ is the aqueous Fe^{2+} concentration remaining after a fraction of

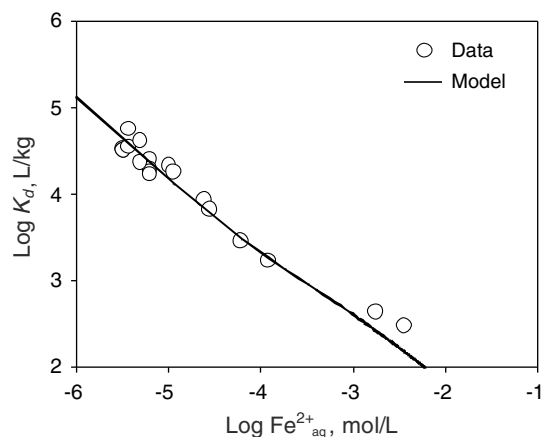


Fig. 6. Fe^{2+} sorption isotherm for conditioned NAu-2 in 0.1 M NaClO_4 expressed as the K_d function (Eq. (2)). The solid line is the model fit to the data.

Fe^{2+} is sorbed to NAu-2 of mass $m_{\text{NAu-2}}$ in the total volume of V . The distribution ratio has the unit of L/kg.

The value of K_d is higher at lower total Fe^{2+} concentration available for sorption (Fig. 6), suggesting a higher sorption affinity. The decreasing K_d value with increasing aqueous Fe^{2+} concentration indicates a nonlinear sorption isotherm. The K_d values decreased markedly to $10^{3.5}$ L/kg with increasing aqueous Fe^{2+} concentration, and decreased more gradually at higher Fe^{2+} concentration, reflecting the effects of mass action and surface site saturation on Fe^{2+} sorption. This value corresponds to 2.0×10^{-1} mol/kg of sorbed Fe^{2+} , equivalent to 24% saturation of the total site density (8.39×10^{-1} mol/kg), as contributed from the amphoteric (1.42×10^{-1} mol/kg) and ion exchange (6.97×10^{-1} mol/kg) site densities.

4. DISCUSSION

4.1. Processes controlling Fe^{2+} sorption

Clay minerals contain two types of sorption sites: pH dependent amphoteric sites which participate in the surface complexation reactions and ionic-strength dependent basal sites which participate in the exchange reactions. The extent and mechanism of sorption exhibited by these two site types in a specific mineral depend on pH, ionic strength and other cations and their selectivity constants (Chisholm-Brause et al., 1994). In most cases both mechanisms operate simultaneously to some extent. The surface complexation reactions involving surface hydroxyl groups at the edge of clay platelets are normally quantified from the sorption isotherms at very low sorbate concentrations and the reaction site densities are characterized by potentiometric titration (e.g., Zachara and McKinley, 1993; McKinley et al., 1995; Baeyens and Bradbury, 1997). Our potentiometric titration results revealed that the protonation/deprotonation reactions are almost independent of ionic strength (Fig. 3). The complexation site density for NAu-2 (141.8 mmol/kg) obtained from the acid end points of the titrations were

higher than that of montmorillonite (80 mmol/kg, Stadler and Schindler, 1993; Baeyens and Bradbury, 1997), kaolinite (79 mmol/kg, Heidmann et al., 2005) and hectorite (92.4 mmol/kg, Schlegel et al., 1999). The substitution of Fe³⁺ in NAu-2 tetrahedral sites (Gates et al., 2002) may have contributed to the higher site density. These data along with the Fe²⁺ adsorption results at pH 4–8 (Fig. 4) which showed a considerable plateau at high ionic strength, are suggestive of Fe²⁺ sorption on amphoteric sites (see also Section 4.3).

The dependence of Fe²⁺ sorption on ionic strength (Fig. 4) is consistent with previous studies (Zachara and McKinley, 1993; Chisholm-Brause et al., 1994; Baeyens and Bradbury, 1997; Schlegel et al., 1999; Dähn et al., 2002). For example, 80% Fe²⁺ sorption occurred in 1 day at 0.1 M of background electrolyte at neutral pH while it took about 15 days at 0.5 M (Fig. 4). After 1-day, Fe²⁺ sorption onto NAu-2, particularly at high ionic strength, increased slowly as a function of time. Our slow sorption results are also similar to Ni sorption onto montmorillonite (Scheidegger et al., 1998) and Co sorption onto hectorite (Schlegel et al., 1999). For example, at low ionic strength (0.01 M), the slow sorption of Co onto hectorite and Fe²⁺ onto nontronite contributed only about 5% of the total sorption in 5 days but did not increase further with additional equilibration time. But at intermediate ionic strength (0.1 M), the sorption of Ni onto montmorillonite and Fe²⁺ onto nontronite continuously increased and contributed 21–25% of total sorption in 35 days.

Metal sorption onto minerals has been suggested to involve up to three different phenomena (or their combination) at the mineral-water interface: non-specific and specific sorption, and dissolution of structural cations followed by their subsequent nucleation (Scheidegger et al., 1998; Schlegel et al., 2001; Dähn et al., 2002; Schlegel and Manceau, 2006). Because cation exchange and surface complexation are fast reactions (e.g., Sposito, 1984; Tang and Sparks, 1993), the slow kinetics of Fe²⁺ sorption in this study suggests the presence of additional mechanisms such as slow surface precipitation and/or nucleation (Sparks, 1989; Scheidegger et al., 1998). This may also include impeded diffusion to or within the interlayers, collapsed edges and other associated micro-fractures in the mineral (Klobe and Gast, 1970; Zachara et al., 2002; Liu et al., 2003), such as fixation to less exchangeable sites in the mineral (Smith and Comans, 1996). In fact, progressive uptake of Fe²⁺ as observed in our study is similar to that of previous studies of Co, Ni and Zn sorption to clay minerals (Schlegel et al., 2001; Dähn et al., 2002; Schlegel and Manceau, 2006). These studies consistently observed increased dissolution in the presence of added metal cations compared to the mineral alone. The rate of metal sorption increased with the presence of other co-precipitants such as Si. Our observation of excess Si dissolution for the experiments in which Fe²⁺ is added (Fig. 1c) is similar to the results as reported by Schlegel et al. (1999) and Schlegel and Manceau (2006). Using P-EXAFS, these authors found that the slow uptake of Co to hectorite and Zn to montmorillonite is a result of nucleation and epitaxial growth of these metals. There-

fore, slow Fe²⁺ sorption kinetics in this study (Fig. 4) is consistent with such a surface nucleation/precipitation mechanism. However, our SEM and XRD analyses were not able to identify any secondary precipitates.

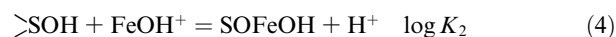
4.2. Effect of dissolved ions on titration and Fe²⁺ sorption

Cations released from limited dissolution of NAu-2 are expected to be the major source of experimental error in the titration experiments. These dissolved cations and their precipitates could contribute to proton consumption/release during the experiments (Baeyens and Bradbury, 1997). Although the amount of structural cations released during the titration experiments (≤ 1.5 h) was small, backward titration (i.e. from neutral pH to acidic or basic and back to neutral) showed a small divergence (data not shown) possibly resulting from dissolution. This hysteresis was apparently stronger at basic than acidic pH (Fig. 3).

Dissolved cations can significantly influence Fe²⁺ sorption to NAu-2 depending on various factors such as pH, cation exchange capacity, and solubility and aqueous speciation of the dissolved constituents (Baeyens and Bradbury, 1997). For example, at the highest and lowest pH (10.7 and 2.8, respectively) used in our experiments, Fe²⁺ sorption reached a maximum after 1 day. With additional equilibration time (≥ 5 days), the extent of sorbed Fe²⁺ gradually decreased. The extent of this decrease was more pronounced at basic than acidic pH (Fig. 5). This result is consistent with the higher extent of dissolution at basic than acidic pH. It is conceivable that the desorption of Fe²⁺ was aided by structurally dissolved cations which compete with Fe²⁺ for available sorption sites on NAu-2.

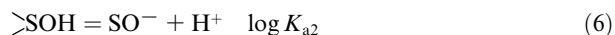
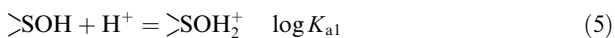
4.3. Modeling

The pH and ionic strength dependence of Fe²⁺ sorption to NAu-2 (Fig. 4) was described with a coupled model of surface complexation and ion exchange reactions using Geochemist's Workbench (Bethke, 2005) and a thermodynamic database compiled by the authors. Similar approaches have been used to simulate divalent metal sorption to clay minerals (e.g., Zachara and McKinley, 1993; McKinley et al., 1995; Turner et al., 1996; Bradbury and Baeyens, 1997), in that surface complexation reactions are used to represent ion sorption on amphoteric edge sites and ion exchange reactions represent ion sorption on fixed charge sites on the basal planes of clay minerals. Two Fe²⁺ surface species, >SOFe^+ and >SOFeOH , that have been used to represent Fe²⁺ surface complexation reactions on iron oxides (e.g., Liger et al., 1999; Liu et al., 2007), were used in our modeling approach:



where >SOH denotes the amphoteric surface site, and K_1 and K_2 are the equilibrium constants for Reactions (3) and (4), respectively.

The protonation state of the amphoteric site was represented by the following two reactions:

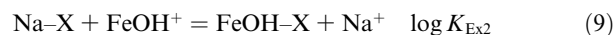


where K_{a1} and K_{a2} are the equilibrium constants. The equilibrium constants for Reactions (5) and (6) were determined by fitting the acid–base titration curves with a non-electrostatic surface complexation model. A site density of 141.8 mmol/kg obtained from titration experiments was used in the surface complexation modeling. The minimal changes of proton consumption/release as a function of electrolyte concentration (Reaction (3)) indicate that a non-electrostatic surface complexation model is sufficient to describe Reactions (5) and (6) under the ionic strength conditions of this study. Parameters K_{a1} and K_{a2} are constrained by the independently measured pH_{PZNPC} (7.2), at which the concentrations of >SOH_2^+ and SO^- are equal by definition. From the mass action equations for Reactions (5) and (6) in the non-electrostatic model, we have $[\text{>SOH}_2^+]/[\text{>SOH}] = K_{a1}\{\text{H}^+\}$ and $[\text{SO}^-]/[\text{>SOH}] = K_{a2}/\{\text{H}^+\}$. Under the condition that the concentrations of >SOH_2^+ and SO^- are the same at the pH_{PZNPC} , the following constraint holds:

$$\log K_{a1} = \log K_{a2} + 2\text{pH}_{\text{PZNPC}} \quad (7)$$

With Eq. (7), only one equilibrium constant (either K_{a1} or K_{a2}) needs to be fitted to describe the acid–base titration results (Fig. 3). Best fits to the experimental data yield $\log K_{a1} = 6.2$ and $\log K_{a2} = -8.2$, and the fitted acid–base titration curves are presented in Fig. 3. In the modeling, the ion exchange between H^+ and Na^+ at the ion exchange site was considered by assuming a unit selectivity coefficient between H^+ and Na^+ (Bradbury and Baeyens, 1997). The proton consumption contributed from the ion exchange reaction was, however, negligible within the titration pH range. The ionic strength has no effect on the calculated titration curve (Fig. 3) due to our use of a non-electrostatic model. The minor increase of the calculated proton consumption near pH 4 at 0.01 M ionic strength is likely due to the ion exchange reaction of H^+ for Na^+ . The model fits the data well below pH 8.0 (Fig. 3). From pH 8.0 to 9.0, however, the model over-estimates proton release, and above pH 9, proton release is under-estimated. The deviation of the model from the experimental data at high pH may also partly result from a subset of amphoteric sites that have different equilibrium constants for the proton release reactions. Similarly, the slight difference in titration data with ionic strength above pH 8.0 might indicate that other unknown reactions may also contribute to the overall proton release. Nevertheless, these differences are small and no attempt was made to consider them in the model. With Reactions (5) and (6) defined, Reactions (3) and (4) were then used to describe Fe^{2+} sorption to the amphoteric site.

The observed effects of ionic strength on Fe^{2+} sorption from pH 4.5 to 8.0 (Fig. 4) indicate that ion exchange reactions are also required to describe Fe^{2+} sorption to NAu-2. Both aqueous species Fe^{2+} and FeOH^+ were considered in order to model the ion exchange reactions:



where X denotes the ion exchange sites, and K_{Ex1} and K_{Ex2} are the conditional selectivity coefficients defined as follows:

$$\frac{N_{\text{Fe-X}_2}\{\text{Na}^+\}^2}{N_{\text{Na-X}}^2\{\text{Fe}^{2+}\}} = K_{\text{Ex1}}, \quad (10)$$

$$\frac{N_{\text{FeOH-X}}\{\text{Na}^+\}}{N_{\text{Na-X}}\{\text{FeOH}^+\}} = K_{\text{Ex2}}, \quad (11)$$

where N is the molar fraction in the exchange phase, and $\{\}$ is the aqueous activity. The cation exchange capacity determined from the NH_4 -exchange method (697 mmol/g) was used in constraining the site balance for the ion exchange reactions. Aqueous activities were calculated using the Davies equation, and aqueous speciation reactions and equilibrium constants were compiled from an available dataset (NIST, 2001). The relevant aqueous speciation reactions are listed in Table 1.

Fe^{2+} sorption Reactions (3), (4), (8) and (9), together with the aqueous speciation reactions (Table 1) and independently determined Reactions (5) and (6), were used to fit Fe^{2+} sorption as a function of pH and ionic strength (Fig. 4). Different combinations of two or three reactions from Reactions (3), (4), (8) and (9) were tried in selecting the minimal number of sorption reactions to best describe the Fe^{2+} sorption to NAu-2. The data for Fe^{2+} sorption at 24 h of equilibration time (Fig. 4) were used to determine the Fe^{2+} sorption reaction constants and the calibrated model was then used to predict the Fe^{2+} sorption isotherm in Fig. 6. The experimental results determined within 24 h of equilibration were used in the modeling because the acid–base titration (Fig. 3) and Fe^{2+} sorption isotherm (Fig. 6) were all measured over this time frame. Fe^{2+} sorption beyond 24 h (Fig. 4) was not modeled because the properties of possible surface precipitates are unknown.

The modeling of Fe^{2+} sorption as a function of pH indicates that Reactions (3), (8) and (9) are required to describe the experimental data, with the best fitted parameters of $\log K_1 = 4.1$, $\log K_{\text{Ex1}} = 1.3$ and $\log K_{\text{Ex2}} = 4.4$. Either Reaction (3) or (4), coupled with Reactions (8) and (9), could describe the data. However, Reaction (3) was ultimately selected because it has been used previously to describe divalent metal sorption to clay minerals (e.g., Zachara and McKinley, 1993; Zachara et al., 1993; McKinley et al., 1995; Turner et al., 1996; Bradbury and Baeyens, 1997). Regardless, a surface complexation reaction is required to describe the sorption edge from pH 3

Table 1
Aqueous speciation reactions

Reactions	$\log K (I = 0)$
$\text{Fe}^{2+} + \text{H}_2\text{O} = \text{FeOH}^+ + \text{H}^+$	-9.4
$\text{Fe}^{2+} + 2\text{H}_2\text{O} = \text{Fe}(\text{OH})_{2(\text{aq})} + 2\text{H}^+$	-20.5
$\text{Fe}^{2+} + 3\text{H}_2\text{O} = \text{Fe}(\text{OH})_3^- + 3\text{H}^+$	-31.0
$\text{Na}^+ + \text{ClO}_4^- = \text{NaClO}_4$	-0.7
$\text{Na}^+ + \text{H}_2\text{O} = \text{NaOH}_{(\text{aq})}$	-13.9

to 4.5. This is in contrast to other divalent metal sorption modeling where the surface complexation reactions primarily contribute to the sorption near neutral pH (e.g., McKinley et al., 1995; Bradbury and Baeyens, 1997). Similarly, Reaction (8) was selected in order to be consistent with previous studies that describe divalent metal sorption as a function of ionic strength from pH 4.5 to 8.0. Reaction (9) was selected to describe the second sorption edge from pH 8.0 to 9.5. Other reactions or combinations of reactions without Reaction (9) were not able to describe the observed Fe²⁺ sorption above pH 8 well. Including FeOH⁺ as an ion exchange species overcomes the effect of aqueous Fe²⁺ hydration at high pH that stabilizes Fe²⁺ in the aqueous phase (Table 1) and accounts for the ionic-strength dependent sorption edges from pH 8.0 to 9.5. Reaction (9) has not been previously considered to describe divalent ion exchange reactions. Without Reaction (9), the calculated Fe²⁺ sorption decreases with increasing pH above pH 8.0, and is dependent on ionic strength. Such sorption decreases with increasing pH above pH 8 have been observed previously for Zn²⁺ and Ni²⁺ (Baeyens and Bradbury, 1997), but not for our Fe²⁺ sorption data (Fig. 4). The reason for this discrepancy between our results for Fe²⁺ and those of Baeyens and Bradbury is unknown.

The model provides a reasonable fit to the observed Fe²⁺ sorption as a function of pH and ionic strength measured within 24 h of equilibration (Fig. 4), except for the deviation below pH 6 in 0.01 M experiments. The calculations suggest that the Fe²⁺ sorption below pH 8 in the high ionic strength solution (0.5 M) was dominated by surface complexation with the extent of surface complexation (plateau between pH 4.5 and 8.0) determined by the amphoteric site density. The excellent match between the calculated and measured plateau of Fe²⁺ sorption between pH 4.5 and 8.0 indicates the importance of Fe²⁺ surface complexation reactions below pH 8.0. In the low ionic strength solution (0.01 M), model simulations suggest that Fe²⁺ sorption is dominated by ion exchange reactions: Reaction (8) at low pH and Reaction (9) at high pH. The deviation at 0.01 M below pH 6 is likely due to the competition of dissolved ions from the dissolution of NAu-2. Dissolved ions, such as Mg²⁺, can conceivably compete with Fe²⁺ at the ion exchange site and thus decrease Fe²⁺ sorption. Such competition would be, however, suppressed at high ionic strengths, leading to a better match between calculated and measured data. At ionic strength 0.1 M, our calculations indicate that both ion exchange and surface complexation contributed to the total Fe²⁺ sorption. Above pH 8, ion exchange (Reaction (9)) dominates Fe²⁺ sorption at all ionic strengths because hydrated aqueous Fe²⁺ species become increasingly important.

The sorption model consisting of Reactions (3), (8) and (9) provides a good fit to the Fe²⁺ sorption data as a function of Fe²⁺ concentration at pH 7.0 (Fig. 6). Model calculations suggest that Fe²⁺ sorption is dominated by surface complexation when aqueous Fe²⁺ is less than 10⁻⁵ mol/L. The amphoteric site then becomes saturated above 10⁻⁵ mol/L Fe²⁺ at pH 7.0, and consequently sorbed Fe²⁺ was dominated by a combination of surface complex-

ation and ion exchange. The calculated slope of K_d vs. aqueous Fe²⁺ concentration gradually decreases to a value of -1 with increasing aqueous Fe²⁺ concentration, consistent with Reaction (3) since sorbed Fe²⁺ becomes independent of aqueous Fe²⁺ concentration as the sorption sites became increasingly saturated.

5. CONCLUSIONS

This study describes Fe²⁺ sorption onto nontronite as a function of ionic strength, pH, Fe²⁺ concentration, and time. All experiments were performed under strictly anoxic conditions (with a Fe²⁺ mass balance of ≥96%), making it possible to collect well constrained and reliable data on Fe²⁺ sorption without complication from Fe²⁺ oxidation. Our sorption results showed both similarities and differences to other studies of divalent cation sorption by clay minerals. Fe²⁺ sorption depends on pH, ionic strength, and Fe²⁺ concentration; and our data required coupled ion exchange and surface complexation reactions for adequate model fits as in previous studies. On the other hand, Fe²⁺ sorption is distinctive in several respects: (1) surface complexation is important to lower pH values than for other divalent cations; (2) an additional sorption edge occurs from pH 7 to 9; and (3) sorption kinetics is important and ionic strength dependent. While the sorption edge from pH 7 to 9 was successfully described with an additional ion exchange reaction that involved a hydrolyzed Fe²⁺ species, further research to directly measure surface Fe²⁺ species is required to resolve the mechanism that led to the increased sorption with increasing pH. The sorption kinetics that continued past 24 h contributed a significant fraction of total Fe²⁺ sorption with the extent of this contribution depending on ionic strength. The kinetic behavior likely results from surface nucleation/precipitation reactions that are promoted by the sorption of Fe²⁺ and other ions derived from NAu-2 dissolution. While such a mechanism is supported by previous studies (Scheidegger et al., 1998; Schlegel et al., 1999; Schlegel and Manceau, 2006), direct measurements using both SEM and XRD analyses were not able to confirm the presence of any secondary precipitates. Independent studies and more sensitive microscopic and spectroscopic techniques are needed to further quantify the reactions and kinetics of Fe²⁺ sorption.

ACKNOWLEDGMENTS

We thank Jennifer Szymanowski from the University of Notre Dame and Wei Seng Ang from Yale University for their help, with the potentiometric titration experiments. This research was supported by grants from National Science Foundation (EAR-0345307) and US Department of Energy (DE-FG02-07ER64369) to H.D. and by DOE Environmental Remediation Science Program (ERSP) for C.L. The research was also supported by small research grants from the Clay Mineral Society (CMS, 2006), Geological Society of America (GSA, 2005), International Association of Mathematical Geology (IAMG, 2006) and Interdepartmental Bateman Postdoctoral Fellowship from Yale University to D.P.J. We thank the AE and anonymous reviewers for their constructive comments which greatly improved the quality of the revised manuscript.

REFERENCES

- Amonette J. E. (2003) Iron redox chemistry of clays and oxides: environmental applications. In *Electrochemical properties of clays, CMS Workshop Lecture* (ed. A. Fitch), Aurora, Clay Mineral Society, pp. 89–148.
- Amram K. and Ganor J. (2005) The combined effect of pH and temperature on smectite dissolution rate under acidic conditions. *Geochim. Cosmochim. Acta* **69**, 2535–2546.
- Anastacio A. S., Fabris J. D., Stucki J. W., Coelho F. S., Pinto I. V. and Viana J. M. (2005) Clay fraction mineralogy of a Cambisol in Brazil. *Hyperfine Interact.* **166**, 619–624.
- Baeyens B. and Bradbury M. H. (1997) A mechanistic description of Ni and Zn sorption on Na-montmorillonite. Part I: titration and sorption measurements. *J. Contam. Hydrol.* **27**, 199–222.
- Bethke C. M. (2005) *Geochemist Workbench Release 6.0*. University of Illinois, Urbana-Champaign.
- Bradbury M. H. and Baeyens B. (1997) A mechanistic description of Ni and Zn sorption on Na-montmorillonite. Part II: modeling. *J. Contam. Hydrol.* **27**, 223–248.
- Bradbury M. H. and Baeyens B. (2005) Modelling the sorption of Mn(II), Co(II), Ni(II), Zn(II), Cd(II), Eu(III), Am(III), Sn(IV), Th(IV), Np(V) and U(VI) on montmorillonite: linear free energy relationships and estimates of surface binding constants for some selected heavy metals and actinides. *Geochim. Cosmochim. Acta* **69**, 875–892.
- Bukka K., Miller J. D. and Shabtai J. (1992) FT-IR study of deuterated montmorillonites: structural features relevant to pillared clay stability. *Clays Clay Miner.* **40**, 92–102.
- Charlet L. and Tournassat C. (2005) Fe(II)–Na(I)–Ca(II) cation exchange on montmorillonite in chloride medium; evidence for preferential clay adsorption of chloride – metal ion pairs in seawater. *Aquat. Geochem.* **11**, 115–137.
- Charlet L., Silvester E. and Liger E. (1998) N-compound reduction and actinide immobilization in superficial fluids by Fe(II): the surface = Fe^{III}OFe^{II}OH species, as major reductant. *Chem. Geol.* **151**, 85–93.
- Chisholm-Brause C., Conradson S. D., Buscher C. T., Eller P. G. and Morris D. E. (1994) Speciation of uranyl sorbed at multiple binding sites on montmorillonite. *Geochim. Cosmochim. Acta* **58**, 3625–3631.
- Dähn R., Scheidegger A. M., Manceau A., Schlegel M. L., Baeyens B., Bradbury M. H. and Morales M. (2002) Neof ormation of Ni phyllosilicate upon Ni uptake by montmorillonite. A kinetics study by powder and polarized extended X-ray absorption fine structure spectroscopy. *Geochim. Cosmochim. Acta* **66**, 2335–2347.
- Dähn R., Scheidegger A. M., Manceau A., Schlegel M. L., Baeyens B., Bradbury M. H. and Chateigner D. (2003) Structural evidence for the sorption of Ni(II) atoms on the edges of montmorillonite clay minerals: a polarized X-ray absorption fine structure study. *Geochim. Cosmochim. Acta* **67**, 1–15.
- Fein J. B., Boily J.-F., Yee N., Gorman-Lewis D. and Turner B. F. (2005) Potentiometric titrations of *Bacillus subtilis* cells to low pH and a comparison of modeling approaches. *Geochim. Cosmochim. Acta* **69**, 1123–1132.
- Fredrickson J. K., Zachara J. M., Kennedy D. W., Kukadappu R. K., Mckinley J. P., Heald S. M., Liu C. and Plymale A. E. (2004) Reduction of TcO₄ by sediment-associated biogenic Fe(II). *Geochim. Cosmochim. Acta* **68**, 3171–3187.
- Furrer G., Zysset M. and Schindler P. W. (1993) Weathering kinetics of montmorillonite: investigations in batch and mixed-flow reactors. In *Geochemistry of Clay–Pore Fluid Interaction*, vol. 4 (eds. D. A. C. Manning, P. L. Hall and C. R. Hughes). Chapman & Hall, London, pp. 243–262.
- Gates W. P., Slade P. G., Manceau A. and Lanson B. (2002) Site occupancies by iron in nontronites. *Clays Clay Miner.* **50**, 223–239.
- Géhin A., Grenèche G.-M., Tournassat C., Brendlé J., Rancourt D. G. and Charlet L. (2007) Reversible surface-sorption-induced electron-transfer oxidation of Fe(II) at reactive sites on a synthetic clay mineral. *Geochim. Cosmochim. Acta* **71**, 863–876.
- Golubev S. V., Bauer A. and Pokrovsky O. S. (2006) Effect of pH and organic ligands on the kinetics of smectite dissolution at 25 °C. *Geochim. Cosmochim. Acta* **70**, 4436–4451.
- Grenthe I., Stumm W., Laaksuharju M., Nilsson A. C. and Wikberg P. (1992) Redox potential and redox reactions in deep groundwater system. *Chem. Geol.* **98**, 131–150.
- Heidmann I., Christl I., Leu C. and Kretzschmar R. (2005) Competitive sorption of protons and metal cations onto kaolinite: experiments and modeling. *J. Colloid Interf. Sci.* **282**, 270–282.
- Hofstetter T. B., Neumann A. and Schwarzenbach R. P. (2006) Reduction of nitroaromatic compounds by Fe(II) species associated with iron-rich smectites. *Environ. Sci. Technol.* **40**, 235–242.
- Horne R. A. (1978) *The Chemistry of Our Environment*. Wiley, New York.
- Jaisi D. P., Kukkadapu R. K., Eberl D. D. and Dong H. (2005) Control of Fe(III) site occupancy on the rate and extent of microbial reduction of Fe(III) in nontronite. *Geochim. Cosmochim. Acta* **69**, 5429–5440.
- Jaisi D. P., Dong H. and Liu C. (2007a) Kinetic analysis of microbial reduction of Fe(III) in nontronite. *Environ. Sci. Technol.* **41**, 2437–2444.
- Jaisi D. P., Dong H. and Liu C. (2007b) Influence of biogenic Fe(II) on the extent of microbial reduction of Fe(III) in clay minerals nontronite, illite, and chlorite. *Geochim. Cosmochim. Acta* **71**, 1145–1158.
- Jaisi D. P., Dong H. and Morton J. P. (2008) Partitioning of Fe(II) in reduced nontronite (NAu-2) to reactive sites: reactivity in terms of Tc(VII) reduction. *Clays Clay Miner.* **56**, 175–189.
- Jeon B.-H., Dempsey B. A., Royer R. A. and Burgos W. D. (2004) Low-temperature oxygen trap for maintaining strict anoxic conditions. *J. Environ. Eng.* **130**, 1407–1413.
- Keeling J. L., Raven M. D. and Gates W. P. (2000) Geology and characterization of two hydrothermal nontronites from weathered metamorphic rocks at the Uley graphite mine, South Australia. *Clays Clay Miner.* **48**, 537–548.
- Klobe W. D. and Gast R. G. (1970) Conditions affecting cesium fixation and sodium entrapment in hydrobiotite and vermiculite. *Soil Sci. Soc. Am. Proc.* **34**, 746–750.
- Kriaa A., Hamdi N. and Srasra E. (2007) Acid–base chemistry of montmorillonitic and beidellitic–montmorillonitic smectite. *Russian J. Electrochem.* **43**, 167–177.
- Lebron I., Suarez D. L., Amrhein C. and Strong J. E. (1993) Size of mica domains and distribution of the adsorbed Na–Ca ions. *Clays Clay Miner.* **41**, 380–388.
- Li Y. L., Vali H., Sears S. K., Yang J., Deng B. and Zhang C. (2004) Iron reduction and alteration of nontronite NAu-2 by a sulfate reducing bacterium. *Geochim. Cosmochim. Acta* **68**, 3251–3260.
- Liger E., Charlet L. and van Cappellen P. (1999) Surface catalysis of uranium (VI) reduction by Fe(II). *Geochim. Cosmochim. Acta* **63**, 2939–2955.
- Liu C., Zachara J. M., Smith S. C., McKinley J. P. and Ainsworth C. C. (2003) Desorption kinetics of radiocesium from subsurface sediments at Hanford Site, USA. *Geochim. Cosmochim. Acta* **67**, 2893–2912.

- Liu C., Zachara J. M., Foster-Mills N. S. and Strickland J. (2007) Kinetics of reductive dissolution of hematite by bioreduced anthraquinone-2,6-disulfonate. *Environ. Sci. Technol.* **41**, 7730–7735.
- Logan B. E., Murano C., Scott K., Gray N. D. and Head I. M. (2005) Electricity generation from cysteine in a microbial fuel cell. *Water Res.* **39**, 942–952.
- May H. M., Kiniburgh D. G., Helmke P. A. and Jackson M. L. (1986) Aqueous dissolution, solubilities and thermodynamic stability of common aluminosilicate clay minerals: kaolinite and smectite. *Geochim. Cosmochim. Acta* **50**, 1667–1677.
- McKinley J. P., Zachara J. M., Smith S. C. and Turner G. (1995) The influence of uranyl hydrolysis and multiple site-binding reactions on adsorption of U(VI) to montmorillonite. *Clays Clay Miner.* **43**, 586–598.
- Merola R. B., Fournier E. D. and McGuire M. M. (2007) Spectroscopic investigations of Fe²⁺ complexation on nontronite clay. *Langmuir* **23**, 1223–1226.
- Metz V., Amram K. and Ganor J. (2005) Stoichiometry of smectite dissolution reaction. *Geochim. Cosmochim. Acta* **69**, 1755–1772.
- NIST (2001) Critically Selected Stability Constants of Metal Complexes Database, Version 6.0 for Windows. US Department of Commerce, Gaithersburg, MD 20899.
- Peretyazhko T. and Sposito G. (2005) Iron(III) reduction and phosphorous solubilization in humid tropical forest soils. *Geochim. Cosmochim. Acta* **69**, 3643–3652.
- Rabung T., Pierret M. C., Bauer A., Geckeis H., Bradbury M. H. and Baeyens B. (2005) Sorption of Eu(III)/Cm(III) on Camontmorillonite and Na-illite. Part I. Batch sorption and time-resolved laser fluorescence spectroscopy experiments. *Geochim. Cosmochim. Acta* **69**, 5393–5402.
- Scheidegger A. M., Strawn D. G., Lamble G. M. and Sparks D. L. (1998) The kinetics of mixed Ni–Al hydroxide formation on clay and aluminum oxide minerals: a time-resolved XAFS study. *Geochim. Cosmochim. Acta* **62**, 2233–2245.
- Schlegel M. L. and Manceau A. (2006) Evidence for the nucleation and epitaxial growth of Zn phyllosilicate on montmorillonite. *Geochim. Cosmochim. Acta* **70**, 901–917.
- Schlegel M. L., Manceau A. and Charlet L. (1999) Sorption of metal ions on clay minerals: 2. Mechanism of Co sorption on hectorite at high and low ionic strength and impact on the sorbent stability. *J. Colloid Interf. Sci.* **220**, 392–405.
- Schlegel M. L., Manceau A., Charlet L., Chateigner D. and Hazemann J. L. (2001) Sorption of metal ions on clay minerals. 3. Nucleation and epitaxial growth of Zn phyllosilicate on the edges of hectorite. *Geochim. Cosmochim. Acta* **65**, 4155–4170.
- Schulthess C. P. and Sparks D. L. (1986) Back titration technique for proton isotherm modeling of oxide surfaces. *Soil Sci. Soc. Am. J.* **50**, 1406–1411.
- Schultz C. and Grundl T. (2004) pH dependence of ferrous sorption onto two smectite clays. *Chemosphere* **57**, 1301–1306.
- Smith J. T. and Comans R. J. (1996) Modeling the diffusive transport and remobilization of ¹³⁷Cs in sediments – the effects of sorption kinetics and reversibility. *Geochim. Cosmochim. Acta* **60**, 995–1004.
- Sparks D. L. (1989) *Kinetics of Soil Chemical Processes*. Academic Press, New York.
- Sposito G. (1984) *Surface Chemistry of Soils*. Oxford University Press, Oxford.
- Stadler M. and Schindler P. W. (1993) Modeling of H⁺ and Cu²⁺ adsorption on calcium-montmorillonite. *Clays Clay Miner.* **41**, 288–296.
- Stookey L. L. (1970) Ferrozine – a new spectrophotometric reagent for iron. *Anal. Chem.* **42**, 779–781.
- Strathmann T. J. and Stone A. T. (2003) Mineral surface catalysis of reactions between Fe(II) and oxime carbamate pesticide. *Geochim. Cosmochim. Acta* **67**, 2775–2791.
- Stucki J. W. (2006) Iron redox processes in clay minerals. In *Handbook of Clay Science* (eds. F. Bergaya, G. Lagaly and B. G. K. Theng). Elsevier, Amsterdam.
- Stucki J. W., Lee K., Zhang L. and Larson R. A. (2002) The effects of iron oxidation state on the surface and structural properties of smectites. *Pure Appl. Chem.* **74**, 2079–2092.
- Stumm W. and Morgan J. J. (1996) *Aquatic Chemistry*. Wiley, New York.
- Stumm W. and Wieland E. (1990) Dissolution of oxides and silicate minerals: rates dependant surface speciation. In *Aquatic Chemical Kinetics* (ed. W. Stumm). Wiley, New York, pp. 367–400.
- Sumner M. E. and Miller W. P. (1996) Cation exchange capacity and exchange coefficients. In *Methods of Soil Analysis*, Soil Science Society of America.
- Tang L. and Sparks D. L. (1993) Cation-exchange kinetics on montmorillonite using pressure-jump relaxation. *Soil Sci. Soc. Am. J.* **57**, 42–46.
- Thompson H. A., Parks G. A. and Brown, Jr., G. E. (1999) Dynamic interactions of dissolution, surface adsorption, and precipitation in an aging cobalt(II)–clay water system. *Geochim. Cosmochim. Acta* **63**, 1767–1779.
- Tournassat C. and Charlet L. (2002) The sorption of ferrous iron onto clay minerals: could aqueous Fe(II) outcompete with radionuclides for immobilization? *Geochim. Cosmochim. Acta* **66**, A783.
- Tournassat C., Greneche J. M. and Charlet L. (2004) Interactions of Fe²⁺, Zn²⁺ and H₄SiO₄ at clay/water interface: distinguishing competitive sorption, co-adsorption and surface oxidation phenomena. *Geochim. Cosmochim. Acta* **68**, A162.
- Turner G. D., Zachara J. M., McKinley J. P. and Smith S. C. (1996) Surface-charge properties and UO₂²⁺ adsorption of a subsurface smectite. *Geochim. Cosmochim. Acta* **60**, 3399–3414.
- Turner D. R., Pabalan R. T. and Bertetti F. P. (1998) Neptunium(V) sorption on montmorillonite: an experimental and surface complexation modeling study. *Clays Clay Miner.* **46**, 256–269.
- Zachara J. M. and McKinley J. P. (1993) Influence of hydrolysis on the sorption of metal cations by smectites: importance of edge co-ordination reactions. *Aquat. Sci.* **55**, 250–261.
- Zachara J. M., Smith S. C., McKinley J. P. and Resch C. T. (1993) Cadmium sorption on specimen and soil smectites in sodium and calcium electrolytes. *Soil Sci. Soc. Am. J.* **57**, 1491–1501.
- Zachara J. M., Smith S. C., Liu C., McKinley J. P., Serne R. J. and Gassman P. L. (2002) Sorption of Cs⁺ to micaceous subsurface sediments from the Hanford site, USA. *Geochim. Cosmochim. Acta* **66**, 193–211.
- Zachara J. M., Heald S. M., Jeon B.-H., Kukkadapu R. K., Dohnalkova A. C., McKinley J. P., Moore D. A. and Liu C. (2007) Reduction of perchlorate by aqueous Fe(II) and the nature of solid phase redox products. *Geochim. Cosmochim. Acta* **71**, 2137–2157.
- Zysset M. and Schindler P. W. (1996) The proton promoted dissolution kinetics of K-montmorillonite. *Geochim. Cosmochim. Acta* **60**, 921–936.